

<https://doi.org/10.1038/s42003-024-06862-7>

Synergistic effects of oxidative and acid stress on bacterial membranes of *Escherichia coli* and *Staphylococcus simulans*



Min Xie¹, Eveline H. W. Koch¹, Cornelis A. van Walree^{1,2}, Ana Sobota³, Andreas F. P. Sonnen⁴, J. Antoinette Killian¹, Eefjan Breukink¹ & Joseph H. Lorent^{1,5} ✉

Oxidative stress in combination with acid stress has been shown to inactivate a wide spectrum of microorganisms, including multi-resistant bacteria. This occurs e.g. in phagolysosomes or during treatment by cold atmospheric pressure plasmas (CAP) and possibly depends on the cell membrane. We therefore explored the effects of CAP-generated reactive oxygen and nitrogen species (RONS) on bacterial growth inhibition and membranes in neutral and acidic suspensions. We observed that growth inhibition was most efficient when bacteria were treated by a mix of short and long-lived RONS in an acidic environment. Membrane packing was affected mainly upon contact with short-lived RONS, while also acidity strongly modulated packing. Under these conditions, Gram-negative bacteria displayed large potassium release while SYTOX Green influx remained marginal. Growth inhibition of Gram-negative bacteria correlated well with outer membrane (OM) permeabilization that occurred upon contact with short and/or long-lived RONS in synergy with acidity. In Gram-positive bacteria, CAP impaired membrane potential possibly through pore formation upon contact with short-lived RONS while formation of membrane protein hydroperoxides was probably involved in these effects. In summary, our study provides a wide perspective on understanding inactivation mechanisms of bacteria by RONS in combination with acidity.

A combination of oxidative and acid stress has been shown to effectively kill bacteria during the innate immune response in phagolysosomes of macrophages and during treatment by cold atmospheric pressure plasma (CAP)^{1–4}. Further, acid and oxidative stress have been shown to enhance the efficacy of certain antibiotics⁵. While there are many studies on the subject, it remains unclear what underlying mechanisms induce this synergy in Gram-positive and Gram-negative bacteria.

As a source for RONS, CAP has become a promising approach to target bacterial infections^{6–11}. The low temperature of CAP, close to human body temperature, makes it applicable to biological tissue such as skin or heat-sensitive surfaces, where it can deliver a reactive cocktail, composed of reactive oxygen and nitrogen species (RONS), electrons, charged particles,

electromagnetic fields and ultraviolet (UV)-light to destroy microorganisms. However, when CAP is generated by a plasma pen and direct contact between the bacterial suspension and the plasma plume is avoided, the resulting antibacterial effect will exclusively originate from solubilized RONS and a decrease of the pH^{3,12}.

CAP has shown the ability to inactivate various kinds of pathogenic bacteria efficiently^{13–15}, but the underlying mechanisms are still under investigation. Generally, the reactive mix of CAP is more active than individual RONS species and relies probably on a synergy of short and long-lived RONS^{3,16}. In plasma-activated solutions, which correspond to indirect treatment, the activity depends on a cocktail of long-lived RONS that are formed^{17,18}. These species alone have a certain antibacterial activity, but their

¹Membrane Biochemistry & Biophysics, Bijvoet Centre for Biomolecular Research, Department of Chemistry, Utrecht University, Utrecht, The Netherlands.

²University College Utrecht, Campusplein 1, Utrecht, The Netherlands. ³Applied Physics Department, Eindhoven University of Technology, Eindhoven, The Netherlands.

⁴Pathology Department, University Medical Center Utrecht, Utrecht, The Netherlands. ⁵Cellular and Molecular Pharmacology, Translational Research from Experimental and Clinical Pharmacology to Treatment Optimization, Louvain Drug Research Institute, UCLouvain, Brussels, Belgium.

✉ e-mail: joseph.lorent@uclouvain.be

potency is enhanced by intramolecular conversions or intermolecular reactions between RONS that can generate short-lived species, and possibly by some synergistic effects on the cells^{12,19}. The antibacterial activity and the half-life of plasma-activated solutions depend strongly on the pH^{3,12,20} and in some cases on the presence of NaCl, for example during oxygen-containing plasma treatment that can generate ClO^- ¹². However, it seems that at acidic pH, a synergy of hydrogen peroxide (H_2O_2), NO_3^- and NO_2^- creates a very high antibacterial activity^{16,17,21}. Interestingly, it is not clear which bacterial components are targeted by this synergistic effect. Since the antibacterial effect depends very much on the bacterial species, it is expected that targets are affected differently.

In this work, to gain a better understanding of the inactivation mechanisms of RONS and acidic stress, we compared the effects of direct versus indirect CAP treatment on Gram-positive and Gram-negative bacteria at both exponential and stationary growth stages at different pHs. As the cell membrane is supposedly one of the main targets of RONS and CAP^{22–25}, we characterized biochemical and biophysical alterations in the cell membrane and established a picture of understanding how the cell membrane is involved in the antibacterial effects of RONS and acidity.

Results

Conditions used throughout this study

Since antibacterial efficiency and the amount of generated RONS by CAP depends on the plasma source, treatment modality as well as the aqueous environment, we aimed to create reproducible treatment conditions.

To achieve this goal, we used the kINPen IND as plasma source and argon as vector gas in a fixed setup which permits continuous agitation of the bacterial suspension through the gas flow and gravity, and hence results in an efficient transfer of RONS into the suspension (Fig. 1). We used the kINPen source because it produces reproducible amounts of RONS and has shown promising results in several clinical studies^{26–28}.

As a treatment modality, we avoided contact with the plasma plume with the bacterial suspension to exclude the effects of the electric field. We further treated samples “directly” or “indirectly”. While direct CAP treatment indicates that the bacterial suspension was subjected to CAP, indirect

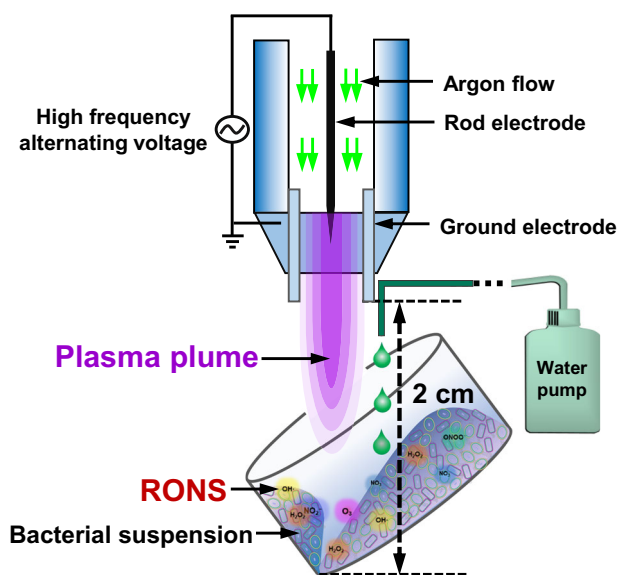


Fig. 1 | Diagram of the experimental setup in this study. The kINPen® IND was used in this study to produce cold atmospheric pressure plasma (CAP) which generates reactive oxygen and nitrogen species (RONS). Argon gas was used as vector gas and the flow rate for CAP generation was 4.2 standard liter per minute (slm). One milliliter of buffer (indirect treatment) or bacterial suspension (direct treatment) was put in the glass beaker and placed under the plasma plume for the indicated treatment time. Milli-Q-H₂O was added continuously to compensate for water evaporation. The distance from the end of the capillary to the bottom edge of the glass beaker was 2 cm (as indicated above).

CAP treatment indicates that the buffer was pretreated for the indicated time interval, and then stored for 2 h before bacteria were incubated in the solution for the indicated time. *Escherichia coli* (MC4100) (*E. coli*) and *Staphylococcus simulans* (*S. simulans*) were selected as representatives of Gram-negative and Gram-positive bacteria, respectively. The large differences in the structure of their bacterial envelope make them interesting choices to compare the activity of CAP on growth and especially on membranes. To prevent any interaction of CAP-generated RONS with organic substances that might interfere with their activity on bacteria and to test the influence of the pH on antibacterial activity, we used inorganic phosphate-buffered saline (PBS) at neutral pH (7.4) and acidic pH (4.5). Testing the efficiency at these pHs is interesting because they mimic the cytoplasmic/exoplasmic (pH = 7.4) or the lysosome's acidity (pH = 4.5). These compartments can be invaded by bacteria or other microorganisms and provoke several types of infection. To fight against these infections, lysosomes and phagolysosomes of neutrophils and macrophages generate a mixture of RONS at pH 4.5 during the so-called oxidative burst. Our experimental conditions could hence give information on the possible synergy of RONS produced by phagolysosomes or CAP, and acid stress. To exclude any changes in pH in our setup, we worked in buffers with fixed pH and checked the pH before and after CAP treatment (Supplementary Fig. 1a).

Inhibition of bacterial growth by CAP depends on the bacterial type, growth phase, acidity, and RONS species

Inhibition of bacterial growth in *E. coli* and *S. simulans* by CAP is summarized in Fig. 2. At both exponential and stationary growth phases, *E. coli* was more susceptible to direct CAP in PBS at acidic pH (Fig. 2a). In addition, CAP was more efficient towards *E. coli* at the exponential growth phase, while indirect CAP treatment had only small effects, that were independent of the pH. In *S. simulans*, acidity enhanced the growth inhibition efficiency of direct CAP, while indirect CAP had no effect. Further, growth inhibition was not significantly influenced when bacteria were either in the stationary or exponential growth phase (Fig. 2b). These observations highlight the difference in susceptibility between Gram-negative and Gram-positive bacteria towards CAP treatment and possibly different mechanisms that lead to the inhibition of growth. Importantly, for both *E. coli* and *S. simulans*, direct CAP efficiently inactivated bacteria under certain conditions while indirect treatment displayed small effects on *E. coli*, suggesting short-lived RONS from CAP dominate bacterial inactivation. As vector gas, argon flow alone was observed to have no significant effects on bacterial growth (Supplementary Fig. 2a).

To assess if the production of certain RONS was related to the acidity of the buffer, we quantified the number of hydrogen peroxides (H_2O_2), hydroxyl radicals ($\text{OH}\cdot$), hypochlorite (ClO^-), nitrite (NO_2^-), and nitrate (NO_3^-) during direct CAP treatment. The production of all species depended on the treatment period (Supplementary Fig. 1b, c and Supplementary Fig. 3). Acidity seemed to reduce the amount of $\text{OH}\cdot$, NO_2^- and slightly ClO^- but not H_2O_2 , while it slightly increased amounts of NO_3^- (Supplementary Fig. 1b, c and Supplementary Fig. 3). Acidity associated with stronger inhibition of growth in *E. coli* and *S. simulans* might hence slightly be influenced by the production of certain RNS such as peroxyxynitrite that can be precursors of NO_3^- production. The influence of hypochlorite on the antibacterial activity was verified by comparing the effects of CAP in a phosphate-buffered NaCl and Na_2SO_4 -containing bacterial suspension. Sodium sulfate prevents the formation of hypochlorite and only a slightly stronger growth inhibition was observed at pH = 7.4 on *S. simulans* in the presence of NaCl while there was no significant difference observed for *E. coli* (Supplementary Fig. 2b).

Antibacterial activity results from additive or synergistic effects of CAP

To obtain a better understanding of which specific RONS dominate the major inactivation effects, we evaluated the inactivation efficiency from individual ROS such as H_2O_2 and $\text{OH}\cdot$ in both neutral and acidic PBSs and

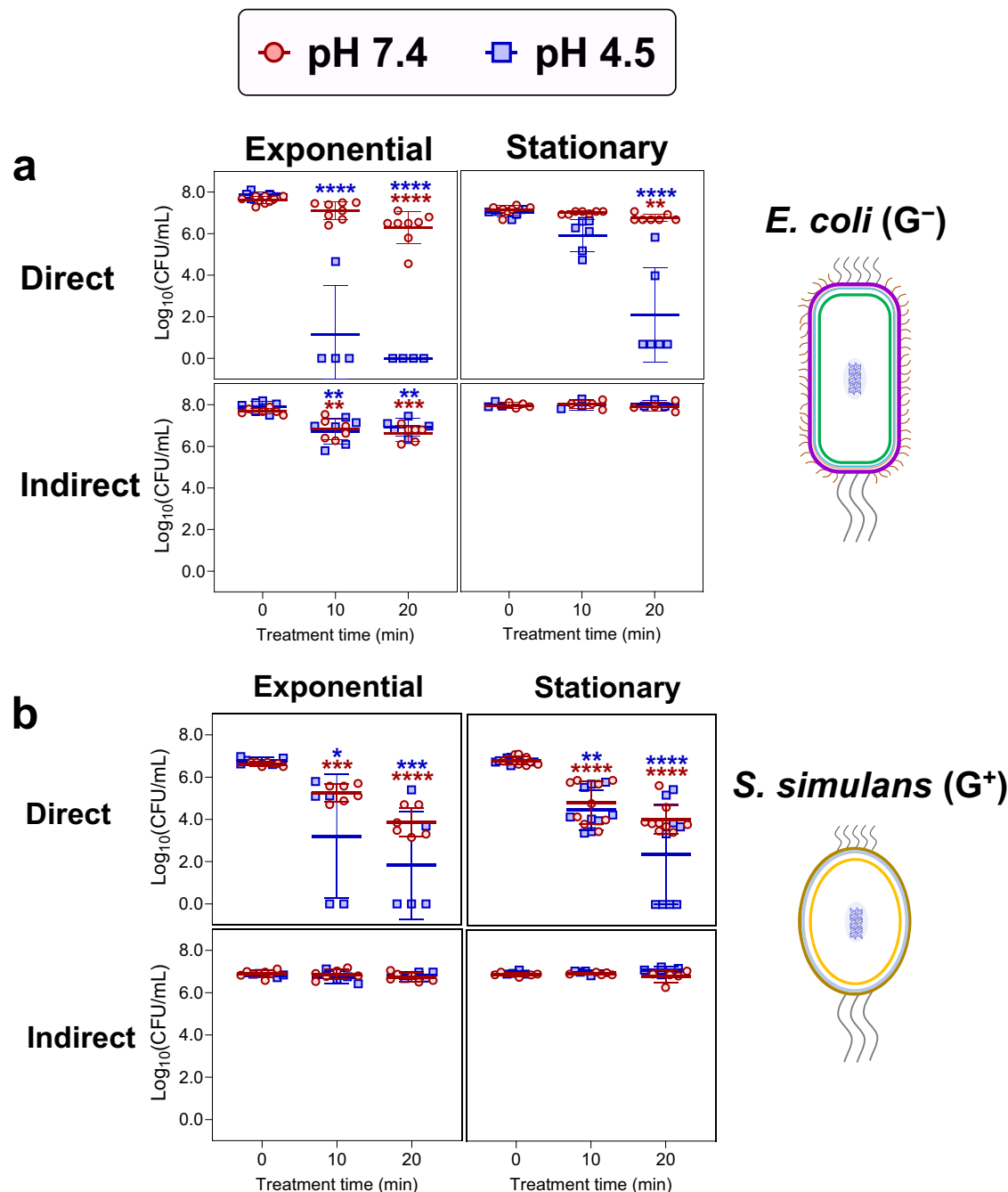


Fig. 2 | Bacterial growth inhibition by CAP. Log_{10} (CFU/ml) colony reduction of **a** *E. coli* and **b** *S. simulans* at exponential and stationary growth phases in PBS at pH = 7.4 (red circles) and pH = 4.5 (blue squares) by direct and indirect CAP, respectively. All experiments were done at least three times independently. Values

are the mean \pm SD ($n \geq 4$). One-way ANOVA analysis was used to compare the difference between treated samples towards corresponding negative controls (* $p < 0.05$, ** $p < 0.01$, *** $p < 0.001$, **** $p < 0.0001$).

compared their activity to CAP-treated PBS containing the same individual ROS concentration. Approximately 400 μM of H_2O_2 were produced in PBS at pH = 7.4 and pH = 4.5 after 20 min CAP treatment, respectively (Supplementary Fig. 1b), during which exponentially grown *E. coli* were reduced by 1.0 ± 0.46 and $7.72 \pm 0.05 \Delta\text{Log}_{10}(\text{CFU/ml})$. In comparison, after 20 min treatment with a similar amount of solely H_2O_2 (Supplementary Fig. 1b), the decrease in bacterial growth was insignificant at both pHs but higher concentrations displayed some activity (Supplementary Fig. 4a). In *S. simulans*, H_2O_2 had no significant effects on growth inhibition, even at far higher concentrations, e.g at 20 mM (Supplementary Fig. 4a). Curiously, the effect of H_2O_2 on *E. coli* was here decreased by acidity but only at concentrations

largely exceeding those obtained during CAP treatment, while no change was observed in *S. simulans*.

Next, we evaluated the killing effects of different mixtures of $\text{H}_2\text{O}_2 + \text{OH}\cdot$ that were produced via the Fenton reaction. The production of $\text{OH}\cdot$ during the Fenton reaction decreased at low pH (Supplementary Fig. 1d). After 20 min of incubation in the $\text{H}_2\text{O}_2/\text{OH}\cdot$ mixture, growth inhibition of *E. coli* was similar to that observed with pure H_2O_2 while *S. simulans* was not inactivated under these conditions (Supplementary Fig. 4b).

The overall inactivation effects in both Gram-positive and Gram-negative bacteria resulted thus from additive or synergistic effects of various

RONS in combination with acidity that are only produced during direct CAP treatment. Since growth inhibition on bacteria was largest in the exponential phase, we characterized the effects on bacterial membranes in exponentially growing bacteria.

CAP, acidity, and argon act differently on membrane packing in *E. coli* and *S. simulans*

Membrane packing influences the function of membrane proteins²⁹, membrane mechanical properties³⁰, and diffusion behavior of certain RONS and other substances through the membrane³¹. A change in lipid membrane packing usually indicates modifications of the membrane lipidome, including lipid oxidation, alterations of transverse lipid monolayer distribution, or other types of changes such as lipid interactions with bivalent cations or protons that can alter the packing of bacterial membranes, e.g. pH with cardiolipin³². We used the polarity-sensitive probes Laurdan and di-4-ANEPPDHQ to detect total membrane packing and outer monolayer membrane packing, respectively^{33,34}. Generalized polarization (GP value) of the polarity-sensitive probes is used here to describe membrane packing³⁵. Generally, a higher GP indicates a decreased polarity of the micro-environment of the fluorophore, meaning less water incursion into the membrane or increased membrane packing.

Our data shows that direct CAP treatment induced significant variations of GP detected with both Laurdan and di-4-ANEPPDHQ compared to untreated samples (Fig. 3a, b). Indirect CAP treatment had only small effects on Laurdan GP in *E. coli* (Supplementary Fig. 5a, b), indicating the importance of short-lived RONS. Interestingly, upon direct CAP treatment Laurdan GP developed in the opposite directions in *E. coli* vs. *S. simulans*, where an increase and a decrease of Laurdan GP were observed, respectively (Fig. 3a). However, for di-4-ANEPPDHQ a decrease in GP was observed in both *E. coli* and *S. simulans* (Fig. 3b). Discrepancies between both probes may be explained by the exclusive outer leaflet location of di-4-ANEPPDHQ which is not the case for Laurdan^{34,36}, by a different location of the probes upon depth along the membrane bilayer axis, and/or by membrane structural differences between Gram-negative and Gram-positive bacteria^{37,38}.

Acidity (pH at 4.5) itself increased GP regardless of bacterial species and probes, suggesting that acidity alone affects bacterial membrane properties. In response to acidic stimuli, bacteria can adjust the fatty acid composition of membrane lipids, such as conversion of unsaturated fatty acids to cyclopropane fatty acids, elongation of acyl chains, and isomerization of fatty acids^{4,39}. However, our data shows that acidity itself did not significantly affect lipid compositional changes of acyl chains after 60 min incubation (Fig. 6d), suggesting that the increased membrane packing in the acid environment was not related to phospholipid composition but probably to protonation of charged lipids such as cardiolipin or LPS at low pH^{32,40}.

Hydrogen peroxide alone influenced Laurdan GP in *E. coli* but only at concentrations above what was observed with CAP, implying that H₂O₂ is most likely not the determining factor in membrane packing in CAP (Supplementary Fig. 5c, d). It is noticeable that the vector gas, i.e. argon stream alone influenced membrane packing in *S. simulans* but not *E. coli* (Supplementary Fig. 5e). We therefore subtracted argon effects from total CAP effects and observed that the effect attributable to RONS was significant in *E. coli* but not *S. simulans* (Supplementary Fig. 5f), suggesting that the observed effects in *S. simulans* may have originated from argon. We note that it has been shown previously that noble gases can affect the order of lipid membrane bilayers and modulate lipid-protein interactions, which is assumed to be one potential mechanism of certain anesthetics^{41–43}.

Species-dependent cytoplasmic release of potassium upon CAP treatment, acidity, and gas flow

Potassium ions (K⁺) are the most abundant inorganic cytoplasmic ions which have crucial roles in bacterial cellular processes. They are mainly implicated in regulating the membrane potential, also during situations of acid or osmotic stress^{44,45}. Membrane potential and the proton-motive force are essential drivers of ATP synthesis through F-ATPases⁴⁶. Abolishing the

membrane potential could hence have catastrophic consequences for bacterial physiology⁴⁷. Potassium ions can generally not diffuse through lipid bilayers due to their positive charge. Its leakage thus indicates membrane disruption, K⁺ channel opening or inhibition of energy-dependent K⁺ transport into the cytosol.

We determined K⁺ release by atomic absorption spectroscopy and our data suggests different modes of K⁺-leakage in *E. coli* and *S. simulans*.

In *E. coli*, direct CAP treatment induced K⁺-leakage which was enhanced under acidic conditions (Fig. 4a, left). Neither indirect CAP treatment (Supplementary Fig. 6a, left) nor Argon itself induced significant K⁺-release (Supplementary Fig. 6b, left), even though it seemed that acidity slightly enhanced K⁺-release (Supplementary Fig. 6a, left).

In *S. simulans*, 10 min of direct CAP treatment already induced nearly 100% of K⁺-leakage in neutral buffer (Fig. 4a, right), moreover, argon (Supplementary Fig. 6b, right) and acidity itself (Fig. 4a and Supplementary Fig. 6b) induced complete K⁺-leakage while indirect CAP did not induce K⁺-leakage (Supplementary Fig. 6a, right).

Membrane potential in *S. simulans* is altered by direct CAP treatment and acidity

Since it is difficult to establish the cytoplasmic membrane potential in Gram-negative bacteria because of their double membrane, we determined membrane potential in *S. simulans* using DiSC₂(5) (3,3'-diethylthiadicarbocyanine, iodide). DiSC₂(5) is a membrane-permeable fluorescent dye that accumulates in cell membranes with intact membrane potential. Accumulation of this dye results in fluorescence self-quenching in the membrane and membrane depolarization induces the release of the dye and thus an increase in fluorescence intensity⁴⁸. In our study, DiSC₂(5) was added into bacterial suspension after various treatment conditions, and the fluorescence intensity upon a time was recorded immediately after its addition (Fig. 4b). Gas flow (e.g., argon and compressed air treatment) alone seemed slightly to influence membrane potential very briefly (Fig. 4b), however, this effect was statistically not significant (Fig. 4c). CAP induced a long-lasting membrane potential depletion and treatment time increased this effect. Acidity itself also affected membrane potential transiently (Supplementary Fig. 6e) while neither indirect CAP nor H₂O₂ affected membrane potential in *S. simulans*. (Supplementary Fig. 6c, d).

Cytoplasmic and outer membrane permeabilization

Bacteria can repair membrane damage to a certain degree in order to keep plasma membrane integrity and thus maintain normal cellular homeostasis⁴⁹, but usually, the formation of larger permanent pores that allow for leakage of larger metabolites and proteins, leads to cell death. To assess if the integrity of the cell envelope was disrupted by CAP, a membrane-impermeable nuclear stain, SYTOX Green was used. The rise of fluorescence indicates membrane pore formation in the cell envelope.

We first excluded the influence of CAP and pH on the SYTOX Green fluorescence since both treatments did not reduce the fluorescence signal of a determined amount of DNA stained by SYTOX Green (Supplementary Fig. 7a). To evaluate if pores were formed after CAP treatment, we washed CAP-treated bacteria with the corresponding buffer at pH = 7.4 and pH = 4.5, respectively, resuspended bacteria with the SYTOX Green solution and observed the SYTOX Green signal for 65 min. We observed that a significant increase in SYTOX Green fluorescence by direct CAP treatment was only observed in *S. simulans*, independently of the pH (Fig. 5a). Interestingly, H₂O₂ at high concentrations was more efficient at permeabilizing plasma membranes of *E. coli* than CAP while it had no effect on *S. simulans* (Supplementary Fig. 7b). In addition, indirect CAP treatment did not induce permeabilization towards SYTOX Green in both bacterial species (Supplementary Fig. 7b). It has to be specified that the H₂O₂ concentrations used here exceed largely H₂O₂ concentration in CAP or physiological situations and can rather be compared to, e.g., concentrations that are used as a topical disinfectant.

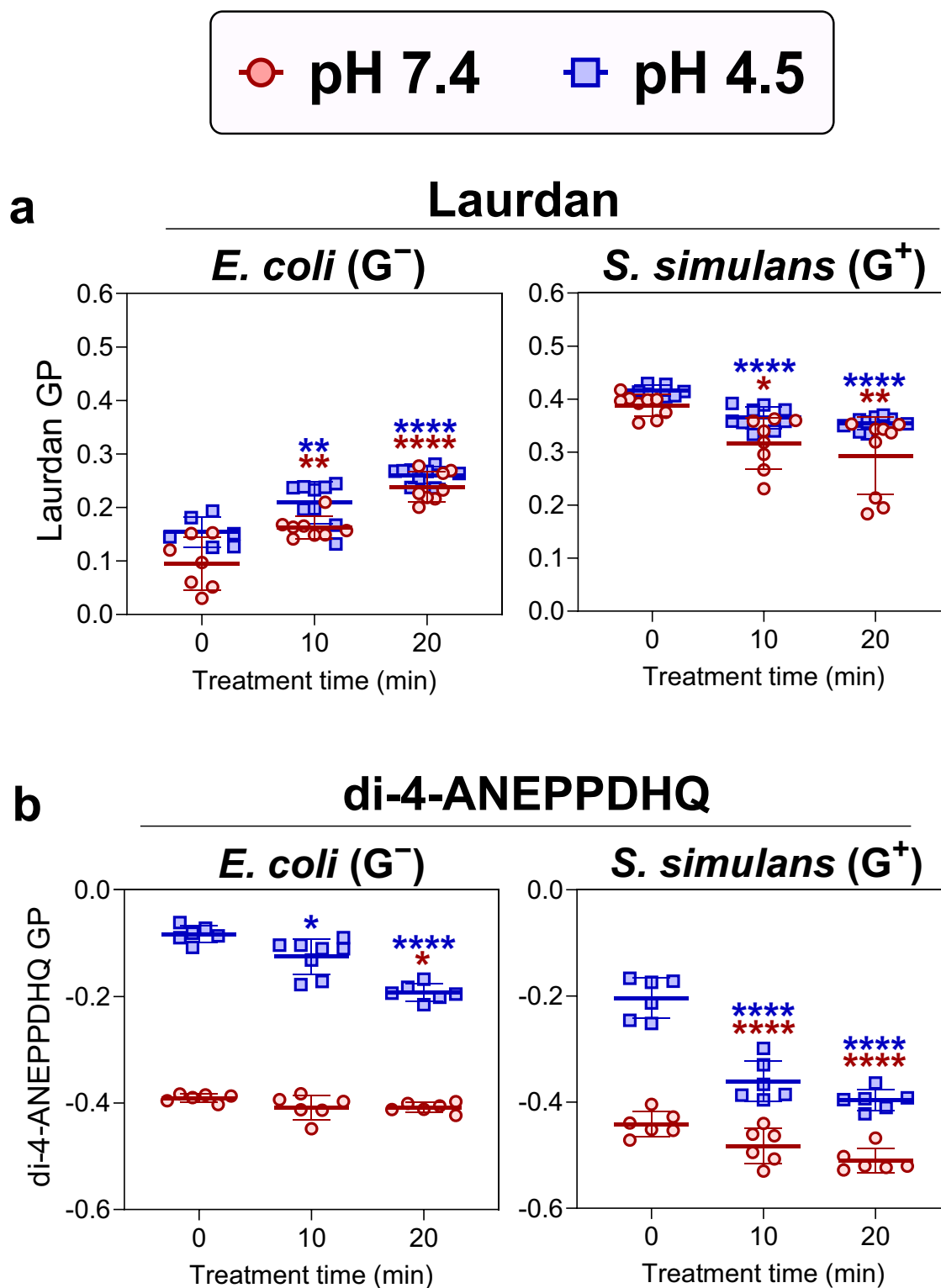


Fig. 3 | Membrane packing is altered by CAP. Membrane packing is determined with (a) Laurdan and (b) di-4-ANEPPDHQ in *E. coli* and *S. simulans* after direct CAP treatment in PBS at pH = 7.4 (red circles) and pH = 4.5 (blue squares). The generalized polarization (GP) values were calculated from two independent

experiments in triplicates. Values are the mean \pm SD ($n \geq 6$). One-way ANOVA analysis was used to compare the difference between CAP-treated samples towards corresponding negative controls (* $p < 0.05$, ** $p < 0.01$, *** $p < 0.001$, **** $p < 0.0001$).

We further assessed outer membrane (OM) permeabilization in *E. coli* by N-phenyl-1-naphthylamine (NPN) uptake^{50,51}. Interestingly, we observed that direct CAP was more efficient in permeabilizing the OM at low pH while indirect CAP and 20 mM H₂O₂ also permeabilized the OM (Fig. 5b and Supplementary Fig. 7c).

Direct CAP induces the formation of membrane protein hydroperoxides only in Gram-positive bacteria

To evaluate the oxidation of membrane components during CAP treatment, we developed a ferrous oxidation-xylenol orange (FOX) assay to detect the formation of lipid and protein hydroperoxides^{52,53}. We first evaluated the

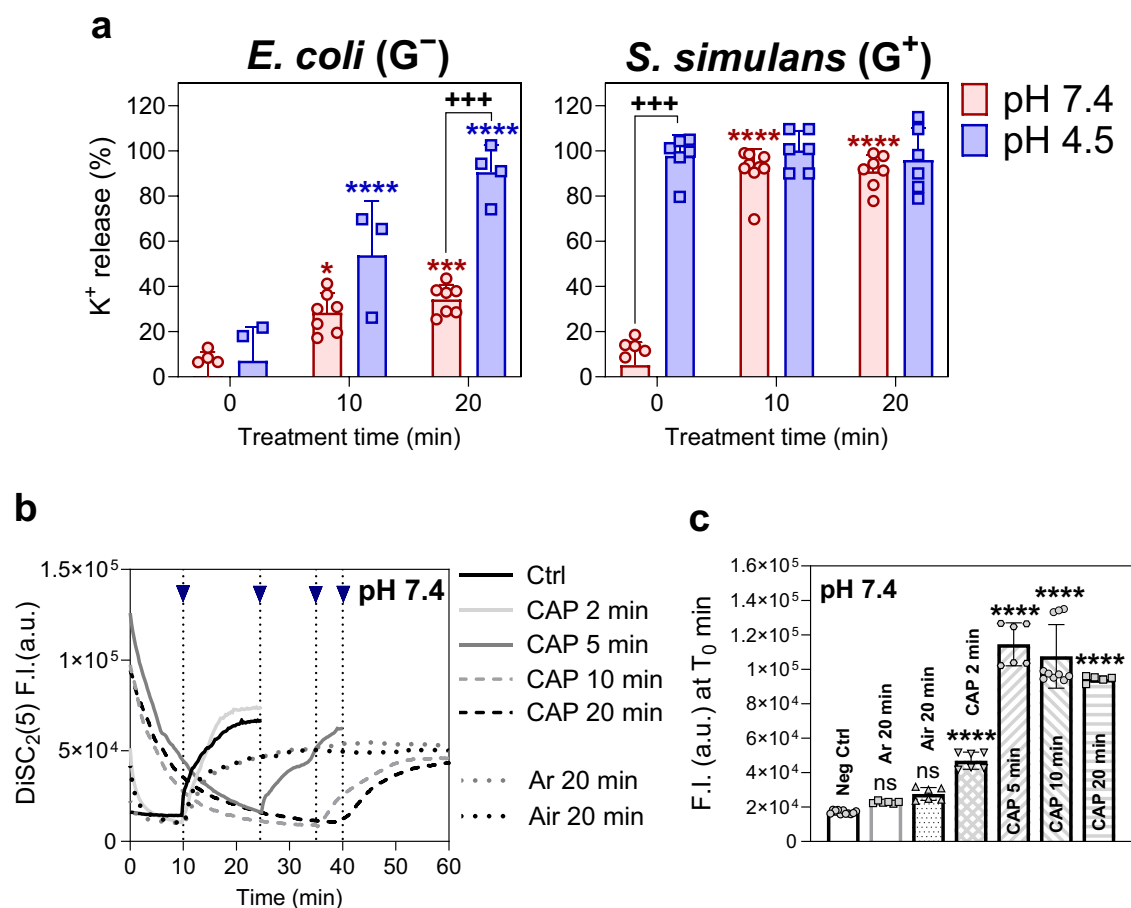


Fig. 4 | Potassium release and membrane potential. **a** Intracellular potassium (K^+) leakage in *E. coli* and *S. simulans* after direct CAP treatment at pH = 7.4 (red circles) and pH = 4.5 (blue squares). **b** Representative membrane potential alteration (in neutral buffer, pH = 7.4) in *S. simulans* after direct CAP, argon or air treatment via a fluorescent dye DiSC₂(5). Arrows indicate the time points when nisin was added to dissipate the membrane potential. **c** Average initial DiSC₂(5) fluorescence upon

different treatments. Potassium (K^+) leakage experiments were performed twice in duplicates. Membrane potential measurements with DiSC₂(5) were conducted twice independently on *S. simulans* at least in triplicates. Values are the mean \pm SD ($n \geq 4$). One-way ANOVA analysis was used to compare the difference between CAP-treated samples towards corresponding controls (+/* $p < 0.05$, ++/* $p < 0.01$, +++/* $p < 0.001$, ++++/* $p < 0.0001$).

assay for protein hydroperoxide formation on bovine serum albumin (BSA) in both neutral and acidic buffers and observed that CAP induced the formation of BSA-derived hydroperoxides (Supplementary Fig. 8).

In *E. coli*, direct CAP treatment did not induce significant hydroperoxide formation in lipids and proteins (Fig. 6a). In *S. simulans*, we observed the formation of hydroperoxides in the protein portion but not in lipids. Protein oxidation was increased upon treatment time and acidity (Fig. 6b). In both bacteria, there was no significant hydroperoxide formation in cytoplasmic proteins (Fig. 6c).

We further investigated if CAP treatment would affect lipid acyl chain composition since oxidation of certain lipids should specifically deplete certain acyl chains and bacteria might adapt their phospholipid composition upon oxidative or acid stress^{39,54}. The acyl chains of membrane lipids in both *E. coli* and *S. simulans* were not significantly altered after direct CAP treatment and H₂O₂ incubation (Fig. 6d and Supplementary Fig. 9).

Discussion

Antibacterial mechanisms of CAP have been widely investigated but no consensus has been reached yet on which underlying mechanisms inactivate bacteria. This is partly due to the large variability in experimental conditions such as different plasma sources, plasma parameters (vector gas, sheath gas), environmental conditions (pH, media), treatment conditions (direct/indirect treatment, distance to plasma plume). In addition to RONS, charged particles, electric fields, and UV radiation might contribute to the antibacterial effects during direct treatment^{55,56}. Nevertheless, the

contribution of other factors than RONS and vector gas atoms (Argon) in our setup is negligible because of the larger distance to the plasma plume (Fig. 1).

To investigate the influence of environmental experimental conditions, we modulated pH and CAP treatment conditions (direct and indirect treatment) on Gram-positive and negative bacteria at different growth phases. We further investigated how the concentration of the generated RONS cocktail would affect bacterial membranes by varying the CAP treatment time (Supplementary Figs. 1 and 3). Testing the effects of a RONS cocktail on bacteria at low pH is particularly interesting since acid stress has been shown to act together with oxidative stress on bacteria during CAP treatment and in phagolysosomes of macrophages. Since the first contact of bacteria with RONS occurs at the cell envelope and since the membrane regulates numerous vital functions, we investigated how CAP-generated RONS in combination with acidity impair membrane functions. Understanding the killing mechanisms related to bacterial membranes should further help to improve the killing efficiency of the RONS cocktail generated by plasma and give potential clues about the effects of the oxidative burst on bacterial membranes in macrophages.

First, our data shows that direct CAP efficiently inhibited growth while indirect CAP treatment had only a small effect on *E. coli* and no effect on *S. simulans*, stressing the importance of short-lived RONS in killing bacteria. Direct CAP treatment has been shown before to be more efficient on bacteria than indirect treatment. Effects are usually attributed to an additive or synergistic effect from short and long-lived RONS, electric fields, or vector

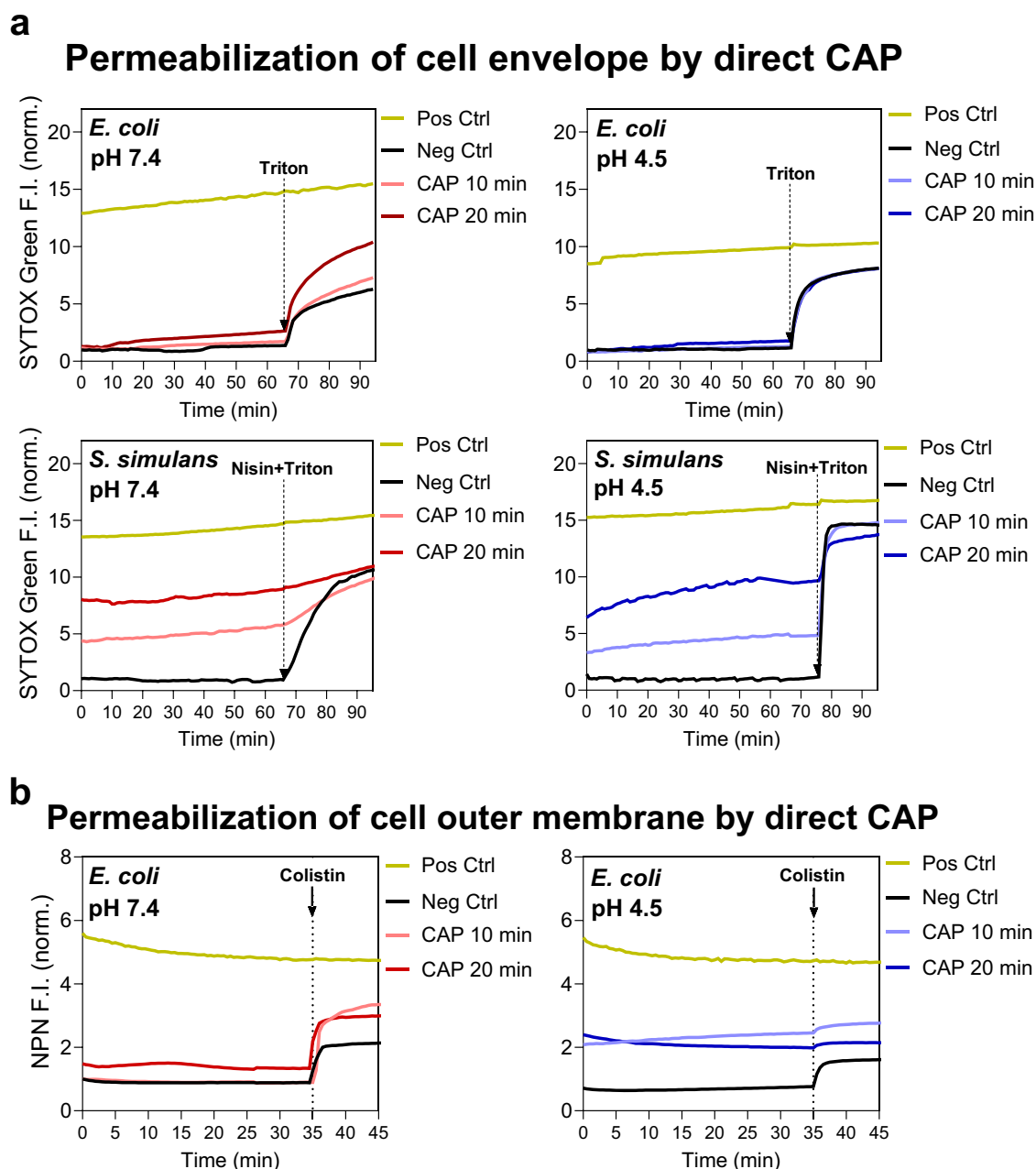


Fig. 5 | Cytoplasmic and outer membrane permeabilization by direct CAP treatment, characterized by SYTOX Green and NPN (N-phenyl-1-naphthylamine), respectively. a Fluorescence intensity of SYTOX Green stained bacterial pellet of *E. coli* and *S. simulans* after direct CAP treatment. Triton X-100 and/ or nisin were used to lyse *E. coli* and *S. simulans* cell suspension (positive controls,

arrows), respectively. **b** Fluorescence intensity of 1-N-phenyl-naphthylamine (NPN) in *E. coli* after direct CAP treatment and 60 min of 150 μM colistin. SYTOX Green permeation into the cytoplasm was determined at least twice independently ($n \geq 3$) while at least three independent experiments were performed for NPN uptake in *E. coli* ($n \geq 9$).

gas ions. Because of our specific setup, the effect of the electric field and the vector gas ions should be negligible in the current study (Fig. 1)⁵⁶. It seems therefore obvious that short-lived RONS are the most efficient antibacterial species here, although we cannot exclude a synergy of short and long-lived RONS since both types of species are generated during direct CAP treatment. Since indirect CAP treatment was able to permeabilize the OM in *E. coli*, it is likely that both short and long-lived reactive species play a role in the inactivation of Gram-negative bacteria. As for *S. simulans* it seems that only short-lived species are effective.

To understand the implications of cell membranes in bacterial inactivation, we performed complementary assays on membrane function. Our results paint a complex picture of the underlying mechanisms in which the effects depended strongly on the bacterial species and acidity.

In *E. coli*, no major formation of lipid or protein hydroperoxides was observed in membranes. Further, there was no significant alteration of lipid acyl chain composition, suggesting there was no major lipid oxidation. However, an effect on the membrane seems obvious since the packing was significantly altered. We cannot exclude that some minor membrane components, such as polyunsaturated isoprenoids that regulate membrane packing, are oxidized and are below the detection limit or not specific to the FOX assay. Lipid peroxidation upon treatment by CAP had been detected in *E. coli* by other groups. However, in these studies the liquid was in direct contact with the plasma plume, suggesting that probably more energetic RONS were formed that might be able to induce lipid oxidation²⁵. Interestingly, potassium release and NPN uptake displayed a strong correlation to growth inhibition upon CAP treatment at low and high pH (Fig. 7a). This

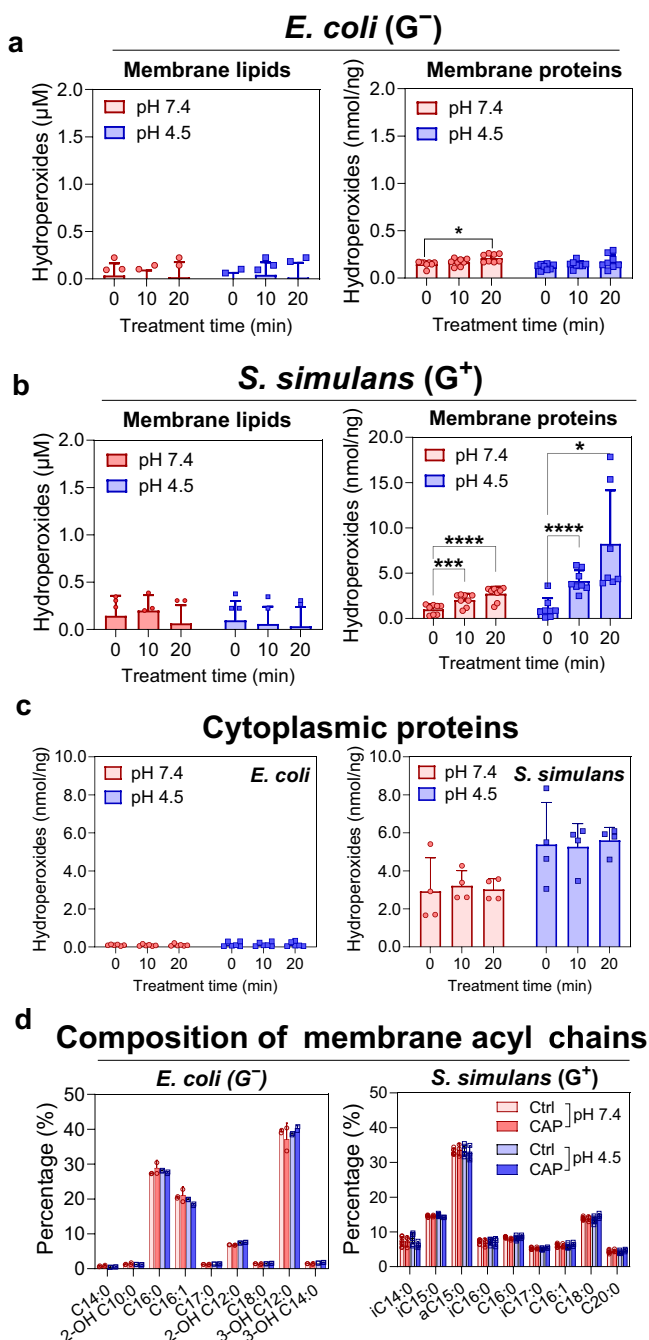


Fig. 6 | Alterations of lipids and proteins by direct CAP. Samples have been treated in PBS at pH = 7.4 (red circles) and pH = 4.5 (blue squares). Membrane hydroperoxide formation of lipids and proteins in **a** *E. coli* and **b** *S. simulans* after direct CAP treatment. **c** Peroxidation of cytoplasmic proteins in *E. coli* and *S. simulans*. **d** Phospholipid acyl chains upon CAP treatment in *E. coli* and *S. simulans*. All experiments were performed twice in duplicates or triplicates. Values are the mean ± SD ($n \geq 6$). One-way ANOVA analysis was used to compare the difference between CAP-treated samples towards corresponding negative controls (* $p < 0.05$, *** $p < 0.001$, **** $p < 0.0001$).

means that OM permeabilization might guide a large part of the effects in *E. coli*. It is interesting to observe that the effects on the OM are also induced by indirect treatment that displayed less growth inhibition on *E. coli* than direct CAP treatment. This could mean that some short-lived species act synergistically with long-lived species on *E. coli* but that short-lived species might have another target than the OM. Acidity increased OM permeabilization during CAP treatment, meaning that either more efficient RONS are

generated that permeabilize the OM, or that the effect of acidity on lipid packing acts synergistically with RONS³². Cytosolic potassium was mainly released upon direct CAP treatment, in a pH-dependent way. This effect did not depend on mechanical stress since Argon treatment was not able to induce K^+ -release in *E. coli*. Curiously, almost no increase in SYTOX Green signal was observed during direct CAP treatment, meaning that either potassium channels and/or pumps were affected, or formation of small membrane pores allowed K^+ to pass but not SYTOX green (Fig. 7b). In a recent publication⁵⁷, we observed immediate K^+ release upon direct CAP treatment in protein-lacking large unilamellar vesicles, pointing to the formation of potassium guiding pores by short-lived RONS in lipid bilayers.

Conversely to *E. coli* we observed the formation of membrane protein hydroperoxides and SYTOX Green influx in *S. simulans*. Interestingly, a strong correlation of growth inhibition with SYTOX Green influx and protein hydroperoxide formation was observed, suggesting that these membrane effects were related to growth inhibition (Fig. 7a). Neither indirect CAP treatment nor H_2O_2 displayed any effect on growth. It seems hence that cytoplasmic membrane permeabilization by short-lived RONS is one of the main mechanisms in Gram-positive bacteria. Regarding biochemical effects on the membrane, we observed significant oxidation of membrane proteins but not lipids upon CAP treatment. In a previous study on the effects of CAP on model membranes composed of unsaturated lipids, in which we used exactly the same treatment conditions, we observed that short-lived RONS were able to induce lipid peroxidation⁵⁷. However, since *S. simulans* are almost devoid of unsaturated acyl chains (Fig. 6d and Supplementary Fig. 9), lipid peroxidation is probably marginal. It remains difficult to imagine how SYTOX Green permeable membrane pores could be formed solely upon oxidation of membrane proteins, but secondary cross-linking of lipids and proteins upon formation of protein hydroperoxides might induce membrane instabilities or permanent pores. Alternatively, other lipid components, that are not detected with our current methods might be oxidized. However, acidity induced complete K^+ release and depolarized the membrane somehow reversibly (Fig. 7c). The synergy of RONS with acidity on growth inhibition might result from this activity and could depend on the opening of K^+ -channels⁴⁴. Argon and air may slightly influence membrane potential but to a far lesser degree than CAP. This might point to a mechanical effect induced by gas flow since Argon and air induced similar effects. CAP-related effects on membrane packing seemed also to depend on the vector gas and not RONS in *S. simulans*. Argon has been shown to induce changes of membrane packing on phospholipid bilayers^{41,43} but since the sample is also agitated by the vector gas flow, alterations in membrane packing or tension, and thus the opening of mechanoreceptors, might be observed⁴⁴. This coincides with the fact that potassium is also released solely upon argon treatment. However, neither argon nor treatment by air had any effect on *S. simulans* viability or SYTOX Green influx but it cannot be excluded that the mechanical effect exerted might have an additive effect on growth inhibition.

Regarding the enhancing effects of acidity on growth inhibition (Fig. 2), it has been speculated that some RONS have a higher activity at low pH. Peroxynitrite ($ONOO^-$), was reported to play a crucial role in CAP-activated water⁵⁸, especially at low pH since its pKa is around 6.8, meaning it can potentially diffuse through membranes to the cytosol in its non-ionized form at low pH. Similarly, the superoxide anion radical ($O_2^{\cdot-}$) has a pKa of 4.88, meaning it would be mainly (~59%) non-ionized at pH = 4.5⁵⁹. In addition to an elevated permeation of RONS through membranes, a low pH could alter the composition of the RONS cocktail as certain reactions in between RONS, or RONS, and biomolecules are favored. We showed that nitrates are preferentially produced at low pH (Supplementary Fig. 3). A similar observation led recently to the conclusion that the formation of peroxynitrite through the reaction $H_2O_2 + H^+ + NO_2^- \rightarrow ONOOH + H_2O$ at low pH could lead to increased antimicrobial effects at low pH⁶⁰. The fact that indirect treatment (Fig. 2) did not have any effect might support this theory since $ONOOH$ has a half-life of seconds and is further degraded into $NO_3^- + H_2O$. Since pH has also an effect on different membrane parameters in both bacteria, it is difficult to pinpoint the

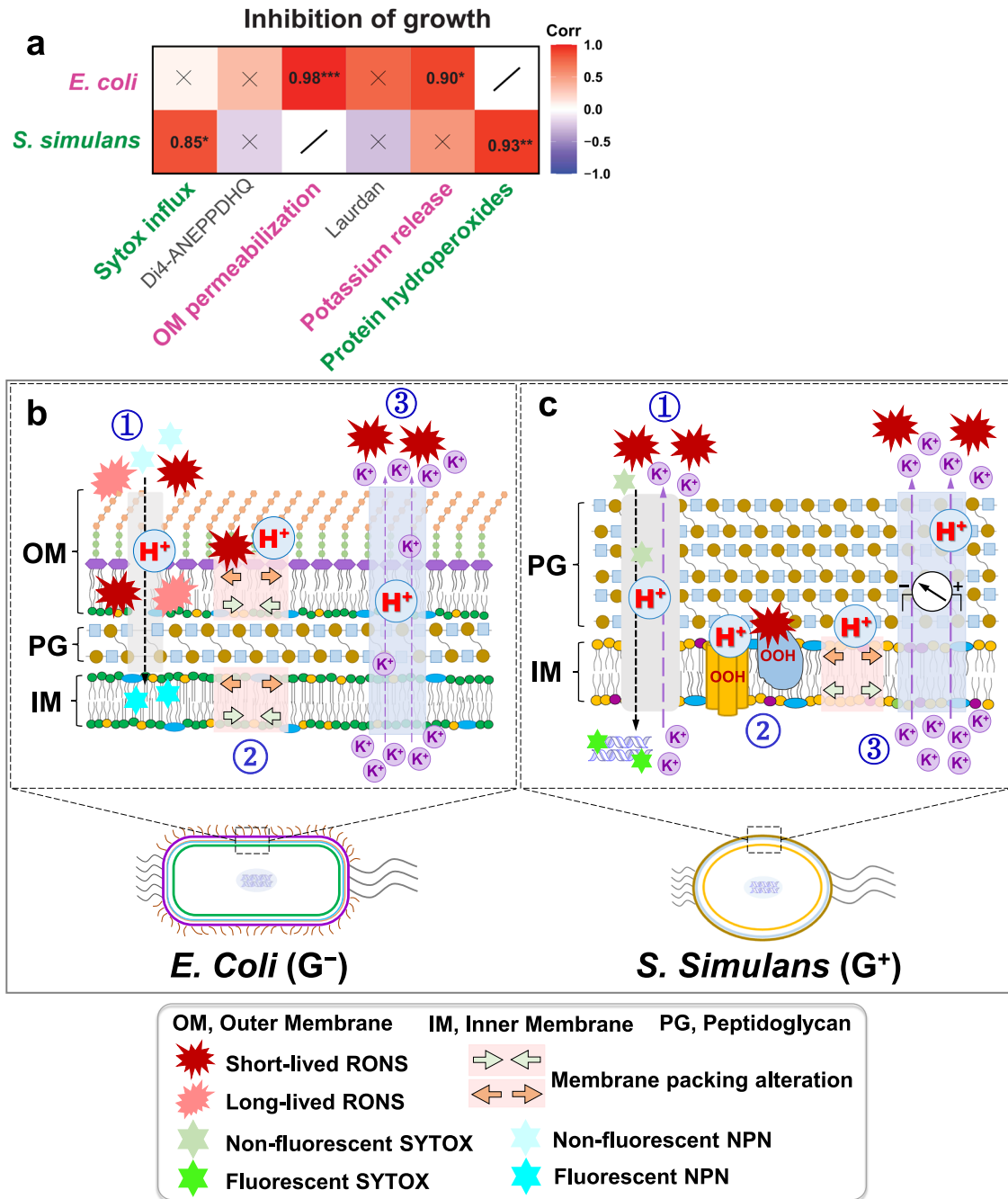


Fig. 7 | Inactivation of Gram-negative (*E. coli*) and Gram-positive (*S. simulans*) bacteria upon CAP treatment. Pearson correlations between alterations of membrane properties and growth inhibition after direct CAP treatment ($*p < 0.05$, $**p < 0.01$, $***p < 0.001$) (a). Schematic diagram of CAP and pH effects on *E. coli* (b) and *S. simulans* (c). ① In *E. coli*, long-lived and probably short-lived RONS from CAP permeabilize the outer membrane in synergy with acidity. ② Acidity strongly alters membrane packing which might lead to a synergistic activity of RONS on the outer membrane. ③ The inner membrane is somehow affected by short-lived RONS

since we observe the release of K^+ mainly upon direct CAP treatment, in a pH-dependent way, although there is neither significant SYTOX influx, nor the formation of lipid or protein hydroperoxides. (c) ① In *S. simulans*, short-lived RONS permeabilize the plasma membrane for larger molecules such as SYTOX Green in a pH-independent way. ② In parallel, the formation of membrane protein hydroperoxides is observed but lipids seem to remain unchanged. ③ Upon the increase of acidity, membrane packing is altered, potassium released and membrane potential dissipated, which might potentiate the inhibition of growth by short-lived RONS.

synergistic origin of RONS and low pH. However, macrophages lower the pH of phagolysosomes during infections probably to exploit the here observed synergistic effects even though differences between the RONS cocktails generated during CAP treatment and in phagolysosomes exist^{28,61–64}. It is difficult to speculate on the precise differences since the concentrations of all RONS haven't been quantified yet in phagolysosomes upon infections, although some species have probably similar concentrations as seen in our setup^{62,63}.

Finally, *E. coli* and other Gram-negative bacteria were more susceptible to oxidative stress in the exponential than in the stationary growth phase while there was no growth phase dependency observed in *S. simulans* and other Gram-positive bacteria^{65,66}. *E. coli* might strengthen its antioxidant defenses in the stationary phase through the σ_S stress response which induces the formation of antioxidant defenses such as catalases that are able to degrade long-lived RONS^{67,68}.

Some bacteria, such as *S. aureus*, have developed multiple mechanisms against oxidative stress that permit them to survive in phagolysosomes and cause recurrent intracellular infections. These mechanisms include the production of antioxidant staphyloxanthins, RONS degrading enzymes such as superoxide dismutase, catalase, or even myeloperoxidase inhibitors that inhibit the production of hypochlorite by the phagosome's myeloperoxidase⁶⁹. Interestingly, it has been shown that CAP is able to promote intraphagolysosomal killing of *S. aureus* in macrophages due to increased intracellular levels of RONS⁷⁰. This suggests that CAP-generated RONS can possibly act in synergy with the oxidative low pH environment in phagolysosomes.

In addition, bacteria can produce biofilms that lead to an intrinsic resistance towards several antibiotics and possibly oxidative stress. The formation of biofilms can lead to a reduction of the effectiveness of CAP since the extracellular matrix can probably partly adsorb oxidative species^{64,71}. Further, it has been shown that *Pseudomonas aeruginosa* biofilms (REF) can increase the production of the antioxidant molecule phenazine that leads to resistance or persistence towards RONS^{64,72}. Nevertheless, it has been shown that most biofilms can be efficiently removed by CAP because it induces the degradation of the biofilm matrix at long term⁷³ and it even increases sensitivity towards commonly used antibiotics⁷⁴.

During the treatment of topical infections by CAP, bacteria can be in direct contact with the plasma plume, which largely increases the antibacterial effect because very short-living vector gas ions, electrons, UV-light, and the electric field act synergistically. Therefore, bacteria that are in contact with the plasma plume are killed within seconds^{25,56}. Since the penetration depth of these very short-living species and the electric field is not very high, bacteria that are situated deeper below the skin surface during profound infections would mainly be in contact with longer-living species. We show in our study that CAP can generate RONS that are able to efficiently kill bacteria but the effect might be mitigated by changes in environmental pH, the growth phase of the bacteria, and certainly the fact that most of the short-living RONS that seem to be essential would not penetrate deeply into the tissue.

In summary, we reveal that an acid environment promotes the killing of bacteria in the presence of complex RONS mixtures produced by CAP in a membrane-dependent fashion (Fig. 7b, c). Further, we show that short-lived RONS are essential to show an effect on plasma membranes at low pH while long-lived RONS alone have an effect on the outer membrane in *E. coli* in a pH-dependent way.

Materials and methods

Chemicals and reagents

Argon (purity 5.0) and oxygen (purity 5.0) were ordered from Linde plc (IRE). Sodium terephthalate (TA) and 2-Hydroxyterephthalate (2-HTA) were ordered from TCI EUROPE N.V. (NL). Hydrogen peroxide solution (Honeywell, 30% w/w), xylene orange tetrasodium salt, and Luria-Bertani (LB) were purchased from Sigma-Aldrich (DE). Di-4-ANEPPDHQ and SYTOX™ Green were ordered from Thermo Fisher Scientific Inc. 1-(6-(dimethylamino) naphthalen-2-yl) dodecan-1-one (Laurdan), 3,3'-Diethylthiadicarbocyanine, iodide (DiSC₂(5)) and Tryptic Soy Broth (TSB) and Nitrite/Nitrate Assay Kit (Roche) were ordered from Merck (USA). The recipe for the different buffers used in this study is shown in Table 1.

Plasma source

For our experiments, we used the kINPen® IND as plasma and RONS source (Fig. 1). It consists of an operating device and a connected hand-held plasma pen. The plasma pen is a needle-type discharge in a dielectric tubing of

0.9 mm inner diameter. Inside, a high electric voltage (2–3 kV) is generated by a high-frequency generator (1 MHz) connected to a metal electrode inside of a ceramic capillary. The vector gas (argon) flow through the capillary is regulated by the operating device. The high-frequency discharge converts the argon gas into CAP. To provide stable and reproducible plasma treatments, the plasma source including argon gas flow is switched on at least 20 min before use. The parameters for plasma jet use are kept constant (gas flow, 4.2 standard liters per minute (slm); Burst on mode) unless stated specifically.

As shown in Fig. 1, the beaker with 1 ml of sample (bacterial suspension for direct treatment or PBS for indirect treatment) was placed under the plasma plume at an angle of 20° between its bottom and the horizontal level. The distance between the exit of the capillary and the bottom of the glass beaker is 2 cm, meaning the plume does not touch the suspension. A water pump containing ultrapure H₂O was used to compensate for water evaporation during treatment. The temperature of the suspension decreased slightly on average by 3 °C below room temperature during CAP treatment.

Bacterial strains and culture conditions

Bacterial strains of *Escherichia coli* (MC4100) and *Staphylococcus simulans* were stored at –80 °C and inoculated in 5 ml of LB (Luria-Bertani) and TSB (Tryptic soy broth) liquid medium in overnight culture, respectively. Bacteria from overnight culture were spread on an LB agar plate and incubated at 37 °C until clear single colonies were observed. A single isolated colony was inoculated in 30 ml LB or TSB liquid medium and cultured at 220 rpm and 37 °C overnight. Afterward, 200 µl of overnight bacterial culture was transferred into 5–30 ml fresh liquid medium until the OD_{600nm} reached the required growth phase. To obtain *E. coli* and *S. simulans* at the exponential growth phase, we harvested bacteria until their growth reached an OD_{600nm} between 0.3 to 0.5. An overnight culture of both bacterial species (OD_{600nm} above 2.0) was used as a stationary growth phase. While inhibition of bacterial growth has been investigated in the exponential and stationary phases, all other experiments were performed in the exponential phase.

Direct CAP treatment on bacteria in suspension

All bacterial cultures were harvested at the required growth phases and washed twice by centrifuging at 4000 × g for 5 min at room temperature. The obtained bacterial pellets were washed twice with PBS and then resuspended and diluted to the required OD_{600nm} with PBS at pH = 7.4 or pH = 4.5. Afterward, 1 ml of each bacterial suspension was treated with CAP for 10 and 20 min (setup is shown in Fig. 1). Bacterial suspensions without any treatments and 20 min argon, air, or pure oxygen flow alone were used as negative controls.

Indirect CAP treatment on bacteria in suspension

One ml of required PBS (pH = 7.4 and pH = 4.5) was pretreated with CAP for 10 and 20 min and then stored at room temperature for another 2 h. Afterward, 5 µl of concentrated bacterial suspension was added to reach the same bacterial concentration as in direct CAP treatment. All the samples were then incubated for another 20 min at room temperature.

Bacterial growth inhibition by H₂O₂ and Fenton reaction

For H₂O₂ treatment, stock H₂O₂ solutions were made in PBS at concentrations of 50 mM, 100 mM, 500 mM, 1 M, and 2 M. Ten microliters of each H₂O₂ stock solution was added into 1 ml of each bacterial suspension, resulting in final H₂O₂ concentrations of 0.5, 1, 2, 5, 10 and 20 mM.

For OH• production, we used ferrous iron (Fe²⁺) and H₂O₂ as reagents for the Fenton reaction (i.e. Fe²⁺ + H₂O₂ → Fe³⁺ + OH• + OH⁻).

Table 1 | Inorganic phosphate buffers with different pHs and salt compositions, used to incubate bacteria with RONS

Buffers	Ingredients
1	50 mM Phosphate (30.38 mM Na ₂ HPO ₄ + 19.62 mM NaH ₂ PO ₄), 150 mM NaCl, pH = 7.4
2	50 mM Phosphate (30.38 mM Na ₂ HPO ₄ + 19.62 mM NaH ₂ PO ₄), 100 mM Na ₂ SO ₄ , pH = 7.4
3	50 mM Phosphate (49.27 mM Na ₂ HPO ₄ + 0.73 mM H ₃ PO ₄), 165 mM, NaCl, pH = 4.5

Hydrogen peroxide was used at the same concentrations as for pure H₂O₂ treatment and added to 1 ml of bacterial suspension. Directly hereafter, ten microliters of 20 mM freshly made Fe₂SO₄ stock solution (made freshly in Milli-Q-H₂O containing 2 mM EDTA) was added, resulting in a final Fe²⁺ concentration of 200 μM.

Quantification of hydrogen peroxide (H₂O₂), hydroxyl radical (OH•), hypochlorite (ClO⁻), nitrite (NO₂⁻) and nitrate (NO₃⁻)

Quantification of H₂O₂ from CAP was determined with FOX assay-1^{75,76} as described below. One ml of PBS (pH = 7.4 and pH = 4.5) was treated with CAP for 5, 10, and 20 min. All treated samples were diluted 100 times with PBS at the same pH. Twenty microliters of each diluted sample was added into 200 μl FOX reagent.

For the quantification of OH• radical produced from direct CAP and Fenton reaction, 4 mM of sodium terephthalate (TA) and its oxidized form, 2-Hydroxyterephthalate (2-HTA), were used⁷⁷. TA can react directly with hydroxyl radicals to produce 2-HTA. The calibration curve was done with 2-HTA, using concentrations from 0 to 100 μM. For the quantification of OH• by direct CAP treatment, one ml of PBS (pH = 7.4 and pH = 4.5) containing TA was treated for 5, 10, and 20 min. For the Fenton reaction, 2 mM of EDTA, 200 μM of FeSO₄ · 7H₂O, and corresponding amounts of H₂O₂ (see Supplementary Fig. 1) were added to 1 ml PBS containing 4 mM TA. Two hundred microliters of each treated sample were transferred into a black 96-well plate with a flat bottom (Nunc) for measurement. Excitation and emission wavelengths at 310 nm and 430 nm were used to determine the fluorescence of 2-HTA using CLARIOstar reader (BMG LABTECH).

For the quantification of ClO⁻ in phosphate-buffered NaCl and Na₂SO₄ after direct CAP treatment, we used the specific reaction between ClO⁻ and 3,3',5,5'-tetramethylbenzidine (TMB)⁷⁸. Specifically, one ml of PBS containing 150 mM NaCl or 100 mM Na₂SO₄ at pH = 7.4 and PBS with 165 mM NaCl at pH = 4.5 were treated with direct CAP for 20 min. Three-hundred microliters of treated PBS above were added to 250 μl of 200 mM sodium acetate-acetic acid (pH = 4.0). Then, 200 μl TMB in ethanol/Milli-Q-H₂O (v/v, 1:1) and 250 μl of Milli-Q-H₂O were added. All the samples were incubated 30 min at room temperature and 200 μl of samples were transferred into a transparent 96-well plate with a flat bottom (Nunc) to take an absorption spectrum from 500 nm to 700 nm with the CLARIOstar reader (BMG LABTECH). The maximum absorbance at 655 nm corresponded to TMB oxidized by ClO⁻.

The concentrations of nitrite (NO₂⁻) and nitrate (NO₃⁻) were determined using a Nitrite/Nitrate Colorimetric Test Kit (Roche). Specifically, one ml of PBS (pH = 7.4 and pH = 4.5) was placed in a beaker and subjected to the direct and indirect treatment of CAP as described above. A hundred microliters of sample, blank or standards for the calibration curve were transferred into two wells of a flat transparent 96-well plate. As blank, 100 μl of Milli-Q-H₂O was used and for the calibration curves, a dilution series of 0.05 mg/l to 5 mg/l NO₂⁻ or NO₃⁻ in Milli-Q-H₂O was made. All samples, blank or standards were then equally treated as described in the protocol of the kit, and absorbance readings for NO₂⁻ and NO₂⁻ + NO₃⁻ were performed sequentially by a CLARIOstar reader at 540 nm.

Bacterial growth inhibition determined by serial dilutions

After treatment (CAP, H₂O₂, Fenton reaction), 20 μl of each treated bacterial sample (OD_{600nm} at 0.05) were transferred into 80 μl of sterilized PBS, resulting in the first five-fold dilution. Five microliters of this bacterial suspension were directly spotted on an agar plate, containing the corresponding growth media. Consecutive five-fold dilutions were then achieved from which 5 μl were spotted each time on LB agar plates. The agar plates were placed in a 37 °C incubator overnight and the resulting colony-forming units (CFU) were counted with *ImageJ*.

Membrane packing

Membrane packing was quantified with polarity-sensitive fluorescent probes Laurdan (6-Dodecanoyl-2-Dimethylaminonaphthalene) and di-4-ANEPPDHQ³⁷.

For Laurdan staining, a stock solution was prepared in ethanol and further diluted in PBS to 500 nM. This solution was diluted with an equal volume of CAP-treated or H₂O₂ incubated bacteria to a final OD_{600nm} of 0.025. The staining process was conducted at 37 °C in the dark for 20 min. The excitation wavelength was 360 nm and emission intensity was scanned from 400 nm to 600 nm. The generalized polarization (GP) was calculated from the equation $GP = (I_{440} - I_{490}) / (I_{440} + I_{490})$, where I₄₄₀ and I₄₉₀ indicate the fluorescence intensity at 440 nm and 490 nm, respectively.

For di-4-ANEPPDHQ (di-4), a similar protocol was established except that the stock solution was prepared in DMSO. Bacteria and probe were diluted to the same concentration and by the same procedure as for Laurdan although staining was conducted at room temperature in the dark for 5 min. The probe was excited at 488 nm and an emission scan was obtained from 520 nm to 740 nm. The generalized polarization (GP) value was calculated from the equation $GP = (I_{560} - I_{620}) / (I_{560} + I_{620})$, where I₅₆₀ and I₆₂₀ corresponded to the fluorescence intensity at 560 nm and 620 nm, respectively.

Potassium (K⁺) ion release assay

One milliliter of bacterial suspension of OD_{600nm} = 0.5 was used for K⁺-release characterization. After the treatments, 400 μl were transferred into a new glass test tube which was later used to determine the intra- and extracellular amount of [K⁺]. The remaining 600 μl were centrifuged at 18,000 × g for 20 min. Then, 400 μl of the supernatant was transferred into another glass test tube which was used to determine the released [K⁺]. The negative control we used was an untreated bacterial sample. All samples were placed on the heater at 150 °C until they were dried completely. Afterward, 100 μl of perchloric acid (70% HClO₄) was added to each sample and heated to 150 °C for 2 h to mineralize all organic material. Finally, 4.8 ml of Milli-Q-H₂O and 100 μl of ammonium hydroxide (25% NH₄OH) were added to each sample to dissolve all the inorganic material and neutralize the solution. The concentration of potassium was measured with Analytik Jena ZEEnit 700 P AAS Atomic Absorption Spectrometer at the potassium band at 766.4908 nm. The calibration curve (0 to 2.5 μg/ml) was made with a stock KCl solution containing the same amount of HClO₄ and NH₄OH to ensure the same measurement conditions as for the samples. The blank consisted of a CAP-treated buffer solution that was submitted to all described procedures. The signal of the blank was subtracted from all samples.

Membrane potential measurement in *S. simulans*

Membrane potential alteration of *S. simulans* was determined with a voltage-sensitive dye 3,3'-Dipropylthiadicarbocyanine iodide (DiSC₂(5))⁴⁸. Exponentially grown *S. simulans* were harvested and washed twice with PBS at pH = 7.4 by centrifuging at 5000 × g for 10 min at room temperature. After incubation with CAP or individual RONS, DiSC₂(5) was added to the bacterial suspension (OD_{600nm} = 0.05) at a final concentration of 1 μM. Two hundred microliters of each sample were transferred into black flat bottom 96-well plates in triplicates. The excitation and emission wavelength for DiSC₂(5) were 610 nm and 660 nm, respectively and fluorescence was recorded immediately after the addition of the dye. Nisin, at 5 μM was used as positive control to completely dissipate the membrane potential.

Permeabilization of the cytoplasmic membrane measured by SYTOX™ Green

Exponentially grown bacteria were suspended at an OD_{600nm} of 2.0 in PBS and submitted to CAP (direct and indirect) treatment and H₂O₂ incubation. As positive lysis controls, we used Triton X-100 at 0.1% for *E. coli* and 0.1% Triton X-100 together with 5 μM nisin for *S. simulans*. The treated bacterial suspension was washed twice with PBS of the same pH by spinning at 5000 g for 10 min. SYTOX Green in PBS was added to bacterial pellets to reach 1 ml of a final concentration of 2 μM. Two hundred microliters of each sample were added into a black 96-well plate (Nunc) with a flat bottom in triplicates and the fluorescence was measured with CLARIOstar reader (BMG LAB-TECH) at 504 nm excitation and 523 nm emission.

Permeabilization of outer membrane measured by N-phenyl-1-Naphthylamine (NPN) uptake

E. coli was harvested at the exponential growth phase and washed with PBS (pH = 7.4) twice by centrifuging at $5000 \times g$ for 5 min. The bacterial pellet was resuspended and diluted to one milliliter of a final OD_{600nm} at 0.5 in PBS (pH = 7.4 or pH = 4.5) for treatment. After treatment, the bacterial suspension was washed twice with the same PBS by centrifuging at $5000 \times g$ for 5 min. Afterward, an NPN stock solution in ethanol was added to each sample, resulting in a final concentration of $10 \mu\text{M}$ ⁷⁹. Two hundred microliters of each sample were added into a black 96-well plate (Nunc) in triplicates. The fluorescence was recorded immediately after the addition of NPN with CLARIOstar reader (BMG LABTECH) by exciting at 350 nm and recording emission at 420 nm. The positive control consisted of incubating bacteria with colistin at $150 \mu\text{M}$ under shaking at 220 rpm and 37 °C for 1 h.

Sample preparation for quantification of lipid and protein hydroperoxides

One milliliter bacterial suspension at final OD_{600nm} of 5.0 in PBS (pH = 7.4 and pH = 4.5) was treated with direct CAP for 10 and 20 min in duplicates. Then, the bacterial sample was washed twice with ultrapure H₂O. Afterward, *E. coli* and *S. simulans* were subjected to continuous sonication on ice for 10 and 20 min, respectively. After sonication, all samples were centrifuged at $260,000 \times g$ for 1 h. The resulting supernatant and pellet were separately transferred into new glass tubes. For the supernatant, 3 ml of chloroform/methanol (v/v, 1:1) mixture was added. After vortexing for 30 s, the mixture was centrifuged for 15 min at $2000 \times g$ and 4 °C. The water phase, containing cytoplasmic proteins, was transferred into a new glass tube. For the pellet, five hundred microliters of ultrapure H₂O were used to resuspend, and then 3 ml of chloroform/methanol (v/v, 1:1) were added. After vortexing for 30 seconds, the mixture was centrifuged for 15 min at $2000 \times g$ and 4 °C. The lower chloroform phase that contains membrane lipids was further transferred to a new glass tube and evaporated by N₂ gas flow. The upper aqueous phase, including the interphase, contains mainly the membrane proteins. All the samples in water phases were frozen at -80 °C and lyophilized until the samples were completely dried. Two hundred microliters of methanol and 200 μl of 5% SDS (freshly in Milli-Q-H₂O) were used to dissolve lipid and protein samples, respectively.

Quantification of lipid and protein hydroperoxides by FOX assay

Because of different solubilities, we employed two different FOX assays, usually referred to as FOX assay-1 and FOX assay-2, to determine protein and lipid hydroperoxides, respectively^{75,76}. In FOX assay-1, all reagents were dissolved in Milli-Q-H₂O while in FOX assay-2, all reagents were dissolved in a methanol/ Milli-Q-H₂O (v/v, 9:1) mixture. Specifically, 25 mM of H₂SO₄ was added firstly in Milli-Q-H₂O and methanol/ Milli-Q-H₂O (v/v, 9:1) mixture to make solvents for FOX assay-1 and FOX assay-2, respectively. Afterward, 100 mM of sorbitol and 4 mM of butylhydroxytoluene (BHT) were added to FOX assay-1 and FOX assay-2, respectively. After vortexing, in both FOX assay-1 and FOX assay-2, 250 μM FeSO₄ and 100 μM xylenol orange were added. Both reagents were vortexed until all the reagents were solubilized completely.

Twenty microliters of extracted proteins and lipids were added into 200 μl of FOX assay-1 and FOX assay-2, respectively. Calibration curves were made separately for both assays with commercial H₂O₂ (Honeywell, 30% (w/w) in H₂O). All the sample mixtures together with standards were vortexed for a few seconds and incubated for 30 min at room temperature in the dark. Afterward, 200 μl were transferred into transparent 96-well plates with a flat bottom (Nunc). The absorbance of all samples was measured at 580 nm using CLARIOstar reader (BMG LABTECH). FOX reagents used in this study were always prepared freshly before use.

Bacterial sample preparation for membrane lipid analysis

For direct CAP treatment, bacterial suspensions were concentrated to a final OD_{600nm} of 10.0 in PBS (pH = 7.4 or pH = 4.5) and 1 ml of this bacterial

suspension was treated for 60 min. For H₂O₂ incubation, ten ml of OD_{600nm} at 1.0 was treated with 200 mM H₂O₂ for 60 min. Before extraction, *S. simulans* was lysed by lysostaphin (1 mg/ml in 20 mM sodium acetate, pH = 4.5) at pH = 7.4 or together with 10 μl of 10 M NaOH at pH 4.5. Afterward, all samples were incubated with lysostaphin for 1 h at 37 °C and shaken at 220 rpm. Membrane lipids were extracted by the Bligh & Dyer method⁸⁰. Finally, chloroform phases were combined, and the mixture dried under N₂ gas at ambient temperature. Hereafter, the lipid extracts were dissolved into 500 μl of methanol and its concentration was determined by a developed Rouser assay⁸¹.

Preparation of fatty acid methyl esters (FAMES)

Analysis of fatty acids by GC was done by making fatty acid methyl esters⁸². Specifically, 100 nmole of lipid extract in chloroform/methanol (v/v, 1:1) was dried with N₂ gas. Five hundred microliter acetone and 750 μl of 2 N sodium methoxide (in methanol) were added to dissolve the dried lipid extracts. After 1 min vortex, 1 ml hexane was added, followed by another 30 seconds vortex. Hereafter, all samples were incubated at room temperature for 8 min and 1 ml acetic acid (0.5 M in Milli-Q-H₂O) was added to stop the reaction, followed by 30 seconds of vortexing. Further, all samples were centrifuged at $2000 \times g$ for 2 min at room temperature. The hexane phase was transferred into a new glass tube and washed with 1 ml Milli-Q-H₂O by vortexing and centrifuging at $2000 \times g$ for 2 min. This process was conducted a few times until the water phase was neutralized. Finally, the hexane phase was dried under N₂ flow and dissolved in 50 μl fresh hexane. All samples were transferred into autosampler vials for gas chromatography analysis.

Lipid acyl chains analysis with gas chromatography (GC)

The FAMES were analyzed by Gas Chromatography-Flame Ionization Detection (GC-FID) on a Trace GC Ultra (Thermo Fisher Scientific) equipped with a biscyanopropyl polysiloxane column (Rt-2560, 100-meter, 0.25 mm ID, 0.2 μm df, Restek, Bellefonte PA) using nitrogen as a carrier gas, at a flow of 1.7 liters per min. Per GC run, 2 μl sample is injected (splitless). The total time per run was 70 min. The GC oven started at a temperature of 40 °C, where it was held for 1 min. Afterwards, the temperature increased to 160 °C with a rate of 10 °C per min, and this process was held for 8 min. Then the temperature increased to 165 °C at a rate of 1 °C per min and this process was held for 6 min. Hereafter the temperature was held at 172 °C for 4 min after a temperature increase of 1 °C per min. This was followed by an increase in temperature to 175 °C at a rate of 1 °C per min. After holding this temperature for 5 min the oven temperature was increased to 200 °C at a rate of 2 °C per min. Hereafter the temperature was ramped with a rate of 10 °C per min where the final temperature of 220 °C was held for 4.5 min.

Peak identification was done using multiple FAME standards (63-B, Nu-Chek-Prep; Bacterial Acid Methyl Esters (BAME) CP Mixture, Matreya LLC; Mixture BR2; 3OH-C12:0; 3OH-C14:0; C10:0; C17:0; C21:0, Larodan).

Statistical analysis

Data were analyzed using GraphPad Prism 10.1.2 version Software and presented as mean \pm SD of at least three independent experiments with replicates or triplicates. The significance of differences was calculated using One-way ANOVA analysis, Two-way ANOVA analysis, and two-tailed unpaired *t*-test. *P*-values lower than 0.05 were considered to indicate a significant difference.

Reporting summary

Further information on research design is available in the Nature Portfolio Reporting Summary linked to this article.

Data availability

The source data underlying the figures can be found in the supplementary data set.

Received: 22 February 2024; Accepted: 6 September 2024;

Published online: 17 September 2024

References

- Sultana, S., Foti, A. & Dahl, J. U. Bacterial defense systems against the neutrophilic oxidant hypochlorous acid. *Infect. Immun.* **88**, e00964-19 (2020).
- Slauch, J. M. How does the oxidative burst of macrophages kill bacteria? Still an open question. *Mol. Microbiol.* **80**, 580–583 (2011).
- Ikawa, S., Kitano, K. & Hamaguchi, S. Effects of pH on bacterial inactivation in aqueous solutions due to low-temperature atmospheric pressure plasma application. *Plasma Process. Polym.* **7**, 33–42 (2010).
- Sohlenkamp, C. In *Biogenesis of Fatty Acids, Lipids and Membranes* (ed. Geiger, O.) 1–13 (Springer International Publishing, Cham, 2017).
- Coulson, G. B. et al. Targeting mycobacterium tuberculosis sensitivity to thiol stress at acidic pH kills the bacterium and potentiates antibiotics. *Cell Chem. Biol.* **24**, 993–1004 (2017).
- Dobrynin, D., Fridman, G., Friedman, G. & Fridman, A. Physical and biological mechanisms of direct plasma interaction with living tissue. *New J. Phys.* **11**, 115020 (2009).
- Bourke, P., Ziuzina, D., Boehm, D., Cullen, P. J. & Keener, K. The potential of cold plasma for safe and sustainable food production. *Trends Biotechnol.* **36**, 615–626 (2018).
- Bárdos, L. & Baránková, H. Cold atmospheric plasma: Sources, processes, and applications. *Thin Solid Films* **518**, 6705–6713 (2010).
- Weltmann, K. D. et al. Atmospheric-pressure plasma sources: prospective tools for plasma medicine. *Pure Appl. Chem.* **82**, 1223–1237 (2010).
- Von Woedtke, T., Metelmann, H.-R. R. & Weltmann, K.-D. D. Clinical plasma medicine: state and perspectives of in vivo application of cold atmospheric plasma. *Contrib. Plasma Phys.* **54**, 104–117 (2014).
- Nosenko, T., Shimizu, T. & Morfill, G. E. Designing plasmas for chronic wound disinfection. *New J. Phys.* **11**, 115013 (2009).
- Kondeti, V. et al. Long-lived and short-lived reactive species produced by a cold atmospheric pressure plasma jet for the inactivation of *Pseudomonas aeruginosa* and *Staphylococcus aureus*. *Free Radic. Biol. Med.* **124**, 275–287 (2018).
- Ziuzina, D., Patil, S., Cullen, P. J., Boehm, D. & Bourke, P. Dielectric barrier discharge atmospheric cold plasma for inactivation of *Pseudomonas aeruginosa* biofilms. *Plasma Med.* **4**, 137–152 (2014).
- Nishime, T. M. C. et al. Non-thermal atmospheric pressure plasma jet applied to inactivation of different microorganisms. *Surf. Coat. Technol.* **312**, 19–24 (2017).
- Klämpfl, T. G. et al. Cold atmospheric air plasma sterilization against spores and other microorganisms of clinical interest. *Appl. Environ. Microbiol.* **78**, 5077–5082 (2012).
- Naitali, M., Kamgang-Youbi, G., Herry, J. M. & Bellon-Fontaine, M. N. Combined effects of long-living chemical species during microbial inactivation using atmospheric plasma-treated water. *Appl. Environ. Microbiol.* **76**, 7662–7664 (2010).
- Kaupe, J. et al. Effect of cold atmospheric plasmas on bacteria in liquid: The role of gas composition. *Plasma Process. Polymers* **16**, e1800196 (2019).
- Iwata, N. et al. Investigation on the long-term bactericidal effect and chemical composition of radical-activated water. *Plasma Process. Polymers* **16**, e1900055 (2019).
- Lukes, P., Dolezalova, E., Sisrova, I. & Clupek, M. Aqueous-phase chemistry and bactericidal effects from an air discharge plasma in contact with water: evidence for the formation of peroxyxynitrite through a pseudo-second-order post-discharge reaction of H₂O₂ and HNO₂. *Plasma Sources Sci. Technol.* **23**, 015019 (2014).
- Ikawa, S., Tani, A., Nakashima, Y. & Kitano, K. Physicochemical properties of bactericidal plasma-treated water. *J. Phys. D: Appl. Phys.* **49**, 425401 (2016).
- Machala, Z. et al. Formation of ROS and RNS in water electro-sprayed through transient spark discharge in air and their bactericidal effects. *Plasma Process. Polym.* **10**, 649–659 (2013).
- Joshi, S. G. et al. Nonthermal dielectric-barrier discharge plasma-induced inactivation involves oxidative DNA damage and membrane lipid peroxidation in *Escherichia coli*. *Antimicrob. Agents Chemother.* **55**, 1053–1062 (2011).
- Kvam, E., Davis, B., Mondello, F. & Garner, A. L. Nonthermal atmospheric plasma rapidly disinfects multidrug-resistant microbes by inducing cell surface damage. *Antimicrob. Agents Chemother.* **56**, 2028–2036 (2012).
- Dezest, M. et al. Oxidative modification and electrochemical inactivation of *Escherichia coli* upon cold atmospheric pressure plasma exposure. *PLoS ONE* **12**, e0173618 (2017).
- Alkawareek, M. Y., Gorman, S. P., Graham, W. G. & Gilmore, B. F. Potential cellular targets and antibacterial efficacy of atmospheric pressure non-thermal plasma. *Int. J. Antimicrob. Agents* **43**, 154–160 (2014).
- Bekeschus, S., Schmidt, A., Weltmann, K. D. & von Woedtke, T. The plasma jet kINPen—a powerful tool for wound healing. *Clin. Plasma Med.* **4**, 19–28 (2016).
- Bekeschus, S. et al. Risk assessment of kINPen plasma treatment of four human pancreatic cancer cell lines with respect to metastasis. *Cancers* **11**, 1237 (2019).
- Reuter, S., Von Woedtke, T. & Weltmann, K. D. The kINPen—A review on physics and chemistry of the atmospheric pressure plasma jet and its applications. *J. Phys. D: Appl. Phys.* **51**, aab3ad (2018).
- Marsh, D. Lateral pressure profile, spontaneous curvature frustration, and the incorporation and conformation of proteins in membranes. *Biophys. J.* **93**, 3884–3899 (2007).
- Kelley, E. G. et al. Scaling relationships for the elastic moduli and viscosity of mixed lipid membranes. *Proc. Natl Acad. Sci. USA* **117**, 23365–23373 (2020).
- Cordeiro, R. M. Reactive oxygen species at phospholipid bilayers: Distribution, mobility and permeation. *Biochim. Biophys. Acta Biomembr.* **1838**, 438–444 (2014).
- Khalifat, N., Fournier, J.-B., Angelova, M. I. & Puff, N. Lipid packing variations induced by pH in cardiolipin-containing bilayers: The driving force for the cristae-like shape instability. *Biochim. Biophys. Acta (BBA)-Biomembranes* **1808**, 2724–2733 (2011).
- Owen, D. M., Rentero, C., Magenau, A., Abu-Siniyeh, A. & Gaus, K. Quantitative imaging of membrane lipid order in cells and organisms. *Nat. Protoc.* **7**, 24–35 (2012).
- Lorent, J. H. et al. Plasma membranes are asymmetric in lipid unsaturation, packing and protein shape. *Nat. Chem. Biol.* **16**, 644–652 (2020).
- Parasassi, T., De Stasio, G., d'Ubaldo, A. & Gratton, E. Phase fluctuation in phospholipid membranes revealed by Laurdan fluorescence. *Biophys. J.* **57**, 1179–1186 (1990).
- Klymchenko, A. S. & Kreder, R. Fluorescent probes for lipid rafts: from model membranes to living cells. *Chem. Biol.* **21**, 97–113 (2014).
- Amaro, M., Reina, F., Hof, M., Eggeling, C. & Sezgin, E. Laurdan and Di-4-ANEPPDHQ probe different properties of the membrane. *J. Phys. D: Appl. Phys.* **50**, 134004 (2017).
- Suhaj, A., Gowland, D., Bonini, N., Owen, D. M. & Lorenz, C. D. Laurdan and Di-4-ANEPPDHQ influence the properties of lipid membranes: a classical molecular dynamics and fluorescence study. *Journal of Physical Chemistry. B* **124**, 11419–11430 (2020).
- Xu, Y. et al. An acid-tolerance response system protecting exponentially growing *Escherichia coli*. *Nat. Commun.* **11**, 1–13 (2020).
- Sturm, M., Gutowski, O. & Brezesinski, G. The effect of pH on the structure and lateral organization of cardiolipin in Langmuir monolayers. *ChemPhysChem* **23**, e202200218 (2022).

41. Chen, J., Chen, L., Wang, Y., Wang, X. & Zeng, S. Exploring the effects on lipid bilayer induced by noble gases via molecular dynamics simulations. *Sci. Rep.* **5**, 17235 (2015).
42. Sierra-Valdez, F. J. & Ruiz-Suárez, J. C. Noble gases in pure lipid membranes. *J. Phys. Chem.* **117**, 3167–3172 (2013).
43. Moskovitz, Y. & Yang, H. Modelling of noble anaesthetic gases and high hydrostatic pressure effects in lipid bilayers. *Soft Matter* **11**, 2125–2138 (2015).
44. Stautz, J. et al. Molecular mechanisms for bacterial potassium homeostasis. *J. Mol. Biol.* **433**, 166968 (2021).
45. Beagle, S. D. & Lockless, S. W. Unappreciated roles for K⁺ channels in bacterial physiology. *Trends Microbiol.* **29**, 942–950 (2021).
46. Kaim, G. & Dimroth, P. ATP synthesis by F-type ATP synthase is obligatorily dependent on the transmembrane voltage. *EMBO J.* **18**, 4118–4127–4127 (1999).
47. Strahl, H. & Hamoen, L. W. Membrane potential is important for bacterial cell division. *Proc. Natl Acad. Sci. USA* **107**, 12281–12286 (2010).
48. te Winkel, J. D., Gray, D. A., Seistrup, K. H., Hamoen, L. W. & Strahl, H. Analysis of antimicrobial-triggered membrane depolarization using voltage sensitive dyes. *Front. Cell Dev. Biol.* **4**, 1–10 (2016).
49. Ammendolia, D. A., Bement, W. M. & Brumell, J. H. Plasma membrane integrity: implications for health and disease. *BMC Biol.* **19**, 71 (2021).
50. Gogry, F. A. et al. Colistin interaction and surface changes associated with mcr-1 conferred plasmid mediated resistance in *E. coli* and *A. veronii* strains. *Pharmaceutics* **14**, 295 (2022).
51. Helander, I. M. & Mattila-Sandholm, T. Fluorometric assessment of Gram-negative bacterial permeabilization. *J. Appl. Microbiol.* **88**, 213–219 (2000).
52. Guéraud, F. et al. Chemistry and biochemistry of lipid peroxidation products. *Free Radic. Res.* **44**, 1098–1124 (2010).
53. Juan, C. A., de la Lastra, J. M., Plou, F. J. & Pérez-Lebeña, E. The chemistry of reactive oxygen species (ROS) revisited: outlining their role in biological macromolecules (DNA, lipids and proteins) and induced pathologies. *Int. J. Mol. Sci.* **22**, 4642 (2021).
54. Lee, T.-H., Hofferek, V., Separovic, F., Reid, G. E. & Aguilar, M.-I. The role of bacterial lipid diversity and membrane properties in modulating antimicrobial peptide activity and drug resistance. *Curr. Opin. Chem. Biol.* **52**, 85–92 (2019).
55. Laroussi, M. & Leipold, F. Evaluation of the roles of reactive species, heat, and UV radiation in the inactivation of bacterial cells by air plasmas at atmospheric pressure. *Int. J. Mass Spectrom.* **233**, 81–86 (2004).
56. Lackmann, J.-W. & Bandow, J. E. Inactivation of microbes and macromolecules by atmospheric-pressure plasma jets. *Appl. Microbiol. Biotechnol.* **98**, 6205–6213 (2014).
57. Xie, M. et al. Two separate mechanisms are involved in membrane permeabilization during lipid oxidation. *Biophys. J.* <https://doi.org/10.1016/j.bpj.2023.10.028> (2023).
58. Zhou, R. et al. Cold atmospheric plasma activated water as a prospective disinfectant: the crucial role of peroxyxynitrite. *Green Chem.* **20**, 5276–5284 (2018).
59. Liu, F. et al. Inactivation of bacteria in an aqueous environment by a direct-current, cold-atmospheric-pressure air plasma microjet. *Plasma Process. Polym.* **7**, 231–236 (2010).
60. Jablonowski, H. et al. Plasma jet's shielding gas impact on bacterial inactivation. *Biointerphases* **10**, 029506 (2015).
61. Bruno, G. et al. On the liquid chemistry of the reactive nitrogen species peroxyxynitrite and nitrogen dioxide generated by physical plasmas. *Biomolecules* **10**, 1687 (2020). Vol. 10, Page 1687.
62. Van Der Heijden, J., Bosman, E. S., Reynolds, L. A., Finlay, B. B. & Isberg, R. R. Direct measurement of oxidative and nitrosative stress dynamics in Salmonella inside macrophages. *Proc. Natl Acad. Sci. USA* **112**, 560–565 (2015).
63. Alvarez, M. N., Peluffo, G., Piacenza, L. & Radi, R. Intrapagosomal peroxyxynitrite as a macrophage-derived cytotoxin against internalized *Trypanosoma cruzi*: consequences for oxidative killing and role of microbial peroxyxynitrite reductases in infectivity. *J. Biol. Chem.* **286**, 6627–6640 (2011).
64. Mai-Prochnow, A. et al. Interactions of plasma-activated water with biofilms: inactivation, dispersal effects and mechanisms of action. *NPJ Biofilms Microbiomes* **7**, 11 (2021).
65. Sies, H. & Jones, D. P. Reactive oxygen species (ROS) as pleiotropic physiological signaling agents. *Nat. Rev. Mol. Cell Biol.* **21**, 363–383 (2020).
66. Haider, M. S., Jaskani, M. J. & Fang, J. in *Biocontrol Agents and Secondary Metabolites* (ed. Jogaiah, S.) 347–382 (Woodhead Publishing, 2021).
67. Wang, C.-H. et al. Prevention of arterial stiffening by using low-dose atorvastatin in diabetes is associated with decreased malondialdehyde. *PLoS ONE* **9**, e90471 (2014).
68. Testerman, T. L. et al. The alternative sigma factor sigmaE controls antioxidant defences required for Salmonella virulence and stationary-phase survival. *Mol. Microbiol.* **43**, 771–782 (2002).
69. Goormaghtigh, F. & Van Bambeke, F. Understanding Staphylococcus aureus internalisation and induction of antimicrobial tolerance. *Expert Rev. Anti Infect. Ther.* **22**, 87–101 (2024).
70. Duchesne, C. et al. Cold Atmospheric plasma promotes killing of *Staphylococcus aureus* by macrophages. *mSphere* **6**, e0021721 (2021).
71. Soler-Arango, J., Figoli, C., Muraca, G., Bosch, A. & Brelles-Mariño, G. The *Pseudomonas aeruginosa* biofilm matrix and cells are drastically impacted by gas discharge plasma treatment: a comprehensive model explaining plasma-mediated biofilm eradication. *PLoS ONE* **14**, e0216817 (2019).
72. Mai-Prochnow, A., Bradbury, M., Ostrikov, K. & Murphy, A. B. *Pseudomonas aeruginosa* biofilm response and resistance to cold atmospheric pressure plasma is linked to the redox-active molecule phenazine. *PLoS ONE* **10**, e0130373 (2015).
73. Gupta, T. T. & Ayan, H. Application of non-thermal plasma on biofilm: a review. *Appl. Sci.* **9**, 3548 (2019).
74. Maybin, J. A. et al. Cold atmospheric pressure plasma-antibiotic synergy in *Pseudomonas aeruginosa* biofilms is mediated via oxidative stress response. *Biofilm* **5**, 100122 (2023).
75. Banerjee, D., Madhusoodanan, U. K., Sharanabasappa, M., Ghosh, S. & Jacob, J. Measurement of plasma hydroperoxide concentration by FOX-1 assay in conjunction with triphenylphosphine. *Clin. Chim. Acta* **337**, 147–152 (2003).
76. DeLong, J. M. et al. Using a modified ferrous oxidation–xylenol orange (FOX) assay for detection of lipid hydroperoxides in plant tissue. *J. Agric. Food Chem.* **50**, 248–254 (2002).
77. Gomes, A., Fernandes, E. & Lima, J. L. F. C. Fluorescence probes used for detection of reactive oxygen species. *J. Biochem. Biophys. Methods* **65**, 45–80 (2005).
78. Guo, Y., Ma, Q., Cao, F., Zhao, Q. & Ji, X. Colorimetric detection of hypochlorite in tap water based on the oxidation of 3,3',5,5'-tetramethyl benzidine. *Anal. Methods* **7**, 4055–4058 (2015).
79. Liu, L. et al. An efficient evaluation system accelerates α -helical antimicrobial peptide discovery and its application to global human genome mining. *Front. Microbiol.* **13**, 870361 (2022).
80. Bligh, E. G. & Dyer, W. J. A rapid method of total lipid extraction and purification. *Can. J. Biochem. Physiol.* **37**, 911–917 (1959).
81. Rouser, G., Fleischer, S. & Yamamoto, A. Two dimensional thin layer chromatographic separation of polar lipids and determination of phospholipids by phosphorus analysis of spots. *Lipids* **5**, 494–496 (1970).
82. Laurentius, T. et al. Long-chain fatty acids and inflammatory markers coaccumulate in the skeletal muscle of sarcopenic old rats. *Dis. Markers* **2019**, 9140789 (2019).

Acknowledgements

We thank the Alliance for financing this project. We thank the help from Roy A. M. van Beekveld and Yang Xu for providing chemicals, suggestions, and bacterial strains. We are grateful to Stephan A. Jonker for assisting with the AAS machine operation. Min Xie was supported by a scholarship from the China Scholarship Council (CSC), <https://www.csc.edu.cn/>, file no. 201809370077.

Author contributions

M.X. and E.H.W.K. performed all the experiments and formal analysis. M.X., C.A.v.W., A.S., A.F.P.S., E.B., J.A.K., and J.H.L. were involved in the conception of the study and the interpretation of results. M.X. and J.H.L. drafted the initial manuscript and all authors contributed to the improvement of this manuscript.

Competing interests

The authors declare no competing interests.

Additional information

Supplementary information The online version contains supplementary material available at <https://doi.org/10.1038/s42003-024-06862-7>.

Correspondence and requests for materials should be addressed to Joseph H. Lorent.

Peer review information *Communications Biology* thanks the anonymous reviewers for their contribution to the peer review of this work. Primary handling editors: Wendy Mok and Tobias Goris.

Reprints and permissions information is available at <http://www.nature.com/reprints>

Publisher's note Springer Nature remains neutral with regard to jurisdictional claims in published maps and institutional affiliations.

Open Access This article is licensed under a Creative Commons Attribution-NonCommercial-NoDerivatives 4.0 International License, which permits any non-commercial use, sharing, distribution and reproduction in any medium or format, as long as you give appropriate credit to the original author(s) and the source, provide a link to the Creative Commons licence, and indicate if you modified the licensed material. You do not have permission under this licence to share adapted material derived from this article or parts of it. The images or other third party material in this article are included in the article's Creative Commons licence, unless indicated otherwise in a credit line to the material. If material is not included in the article's Creative Commons licence and your intended use is not permitted by statutory regulation or exceeds the permitted use, you will need to obtain permission directly from the copyright holder. To view a copy of this licence, visit <http://creativecommons.org/licenses/by-nc-nd/4.0/>.

© The Author(s) 2024